

Detecting the Cosmic Gravitational Wave Background with the Big Bang Observer

Vincent Corbin and Neil J. Cornish

Department of Physics, Montana State University, Bozeman, MT 59717

Abstract

The detection of the Cosmic Microwave Background Radiation (CMB) was one of the most important cosmological discoveries of the last century. With the development of interferometric gravitational wave detectors, we may be in a position to detect the gravitational equivalent of the CMB in this century. The Cosmic Gravitational Background (CGB) is likely to be isotropic and stochastic, making it difficult to distinguish from instrument noise. The contribution from the CGB can be isolated by cross-correlating the signals from two or more independent detectors. Here we extend previous studies that considered the cross-correlation of two Michelson channels by calculating the optimal signal to noise ratio that can be achieved by combining the full set of interferometry variables that are available with a six link triangular interferometer. In contrast to the two channel case, we find that the relative orientation of a pair of coplanar detectors does not affect the signal to noise ratio. We apply our results to the detector design described in the Big Bang Observer (BBO) mission concept study and find that BBO could detect a background with $\Omega_{gw} > 2.2 \times 10^{-17}$.

I. INTRODUCTION

Most theories describing the formation of the Universe (Inflation, Qflation, etc.) predict that processes in the early Universe will lead to the copious production of gravitational waves. The detection of such a cosmic gravitational background (CGB) would allow us to probe the earliest moments in the history of the Universe, and place strong constraints on the competing theories [1]. However, detecting the CGB will not be easy since it will be hidden behind the signals from astrophysical sources (binaries systems...) and buried in the instrumental noise. Our current understanding of compact binary systems suggests that there is a window above 0.1 Hz where the number of astrophysical sources is small enough that their contribution can be isolated and removed from the detector data streams [2, 3]. The CGB signal can then be dug out of the instrument noise by cross-correlating the outputs of two or more independent detectors [4, 5]. The Big Bang Observer (BBO) [6] has been proposed as a future space based mission designed to operate in the range $0.1 \rightarrow 1$ Hz. The BBO proposal calls for a fleet of triangular interferometers operating on the same principle as the Laser Interferometer Space Antenna (LISA). The BBO detectors will be ~ 100 times smaller than the LISA detector, and will be considerably more sensitive. It is possible to synthesize three independent data channels [7] (labeled (A, E, T)) in each detector. In principle one could cross correlate these channels using data from a single detector as the channels are nominally noise orthogonal. However, the A and E channels are also signal orthogonal, and the T channel has poor sensitivity to waves with wavelengths larger than the detector. Moreover, the three channels are constructed from links that share common noise sources, so it will be difficult to achieve exact noise orthogonality in practice. The BBO design overcomes these obstacles by employing multiple detector units. A pair of co-planar detectors yields the greatest sensitivity as the antenna patterns have significant overlap. The BBO design also calls for two widely separated “outrigger” constellations that give enhanced angular resolution for detecting astrophysical sources [8], but the wide separation ($\sqrt{3}\text{AU} = 866$ sec) renders them useless for performing cross correlated detection of the CGB in the $0.1 \rightarrow 1$ Hz range.

Here we study the optimal cross correlation of co-planar triangular interferometers. This work generalizes earlier studies [9, 10, 11] that only considered the cross correlation of two Michelson channels. By cross-correlating all possible combinations of the A, E, T channels

in the two detectors the overall sensitivity is improved by a factor of $\sqrt{2}$ at low frequencies and by a factor of $\sqrt{3}$ at high frequencies. In contrast to the single channel case [11], the optimal sensitivity is independent of the relative angle between the two co-planar detectors. We find that the fiducial BBO design [6] will permit the detection of a scale invariant CGB with $\Omega_{gw} = 2.2 \times 10^{-17}$ at 95% confidence.

We begin in Section II by describing the gravitational wave response of the A , E and T channels. This is followed in Section III by a calculation of the noise transfer functions in each channel. Section IV describes the optimal cross correlation of the independent data channels in a pair of co-planar detectors. Section V covers the numerical evaluation of the overlap functions and a calculation of the optimal BBO sensitivity. We use geometric units with $G = c = 1$.

II. DETECTOR RESPONSE

The noise orthogonal data channels A , E and T are formed from linear combinations of the three Sagnac channels s_1, s_2, s_3 :

$$A = \frac{1}{\sqrt{2}}(s_3 - s_1) \quad E = \frac{1}{\sqrt{6}}(s_1 - 2s_2 + s_3) \quad T = \frac{1}{\sqrt{3}}(s_1 + s_2 + s_3) \quad (1)$$

The Sagnac interferometer measures the phase difference of two laser beams starting from the same location and going around the triangle formed by the three spacecraft, one traveling clockwise, the other counterclockwise. Ideally the phase difference is due only to the variations of the interferometer arms' length caused by the gravitational waves. Therefore if the beams start from spacecraft 1, the signal is simply

$$s_1(t) = \frac{1}{3L} [l_{13}(t - 3L) + l_{32}(t - 2L) + l_{21}(t - L) - l_{12}(t - 3L) - l_{23}(t - 2L) - l_{31}(t - L)], \quad (2)$$

where $l_{ij}(t - nL)$ is the distance at time $t - nL$ between spacecraft i and j and L is the length of the interferometer arms (assuming all the arms have the same length). For a plane gravitational wave propagating in $\hat{\Omega}$ direction, this can be shown [11] to reduce to

$$s_1(t) = \mathbf{D}_s(\vec{a}_1, \vec{b}_2, \vec{c}_3, \hat{\Omega}, f) : \mathbf{h}(f, t, \vec{x}_1), \quad (3)$$

where $\vec{a}_1, \vec{b}_2, \vec{c}_3$ are vectors that point along the interferometer arms, $\mathbf{h}(f, t, \vec{x}_1)$ is the tensor describing the wave in the transverse-traceless gauge at point \vec{x}_1 ,

$$\mathbf{D}(\vec{a}_1, \vec{b}_2, \vec{c}_3, \hat{\Omega}, f) = \frac{1}{6} \left(\vec{a} \otimes \vec{a} T_1(f, \vec{a}) + \vec{b} \otimes \vec{b} T_2(f, \vec{b}) + \vec{c} \otimes \vec{c} T_3(f, \vec{c}) \right) \quad (4)$$

and

$$T_1(\vec{a}, f) = e^{-if_n(1+\vec{a}\cdot\hat{\Omega})} \text{sinc}\left(f_n(1+\vec{a}\cdot\hat{\Omega})\right) - e^{-if_n(5+\vec{a}\cdot\hat{\Omega})} \text{sinc}\left(f_n(1-\vec{a}\cdot\hat{\Omega})\right), \quad (5)$$

$$T_2(\vec{b}, f) = e^{-if_n[3+(\vec{a}-\vec{c})\cdot\hat{\Omega}]} \left[\text{sinc}\left(f_n(1+\vec{b}\cdot\hat{\Omega})\right) - \text{sinc}\left(f_n(1-\vec{b}\cdot\hat{\Omega})\right) \right], \quad (6)$$

$$T_3(\vec{c}, f) = e^{-if_n(5-\vec{c}\cdot\hat{\Omega})} \text{sinc}\left(f_n(1+\vec{c}\cdot\hat{\Omega})\right) - e^{-if_n(1-\vec{c}\cdot\hat{\Omega})} \text{sinc}\left(f_n(1-\vec{c}\cdot\hat{\Omega})\right), \quad (7)$$

with $f_n = \pi L f$. Similarly the Sagnac signal extracted at vertex 2 and 3 can be found from symmetry by rotating the system:

$$s_2(t) = \mathbf{D}_s(\vec{c}_1, \vec{a}_2, \vec{b}_3, \hat{\Omega}, f) : \mathbf{h}(f, t, \vec{x}_2),$$

$$s_3(t) = \mathbf{D}_s(\vec{b}_1, \vec{c}_2, \vec{a}_3, \hat{\Omega}, f) : \mathbf{h}(f, t, \vec{x}_3). \quad (8)$$

We are now ready to find the A , E and T detector responses to a plane gravitational wave. To simplify matters we write the signal in the form

$$s_n(t) = \mathbf{D}_n(\hat{\Omega}, f) : \mathbf{h}(f, t, \vec{x}_0), \quad (9)$$

with

$$\mathbf{D}_n(\hat{\Omega}, f) = \vec{a} \otimes \vec{a} T_n^a + \vec{b} \otimes \vec{b} T_n^b + \vec{c} \otimes \vec{c} T_n^c. \quad (10)$$

We define our reference point \vec{x}_0 to be the center of the triangle, and write

$$\mathbf{h}(f, t, \vec{x}) = e^{-i2\pi f \hat{\Omega} \cdot (\vec{x} - \vec{x}_0)} \mathbf{h}(f, t, \vec{x}_0). \quad (11)$$

The T variable, which is also called the symmetrized Sagnac, has an obvious cyclic symmetry:

$$T_T^a = T_T^b = T_T^c = T_T, \quad (12)$$

where

$$T_T(\vec{u}_2 \cdot \hat{\Omega}, f) = \frac{e^{-i\frac{f_n}{3}(9+(\vec{u}_1-\vec{u}_3)\cdot\hat{\Omega})}}{6\sqrt{3}} \left(1 + 2 \cos(2f_n) \right) \left[\text{sinc}\left(f_n(1+\vec{u}_2\cdot\hat{\Omega})\right) - \text{sinc}\left(f_n(1-\vec{u}_2\cdot\hat{\Omega})\right) \right] \quad (13)$$

The variable A , on the other hand, does not have this nice symmetry:

$$T_A(\vec{a} \cdot \hat{\Omega}, f) = \frac{-i}{3\sqrt{2}} \sin(f_n) e^{-i\frac{f_n}{3}(6+(\vec{c}-\vec{b})\cdot\hat{\Omega})} \left[\text{sinc}\left(f_n(1+\vec{a}\cdot\hat{\Omega})\right) + e^{-2if_n} \text{sinc}\left(f_n(1-\vec{a}\cdot\hat{\Omega})\right) \right], \quad (14)$$

$$T_A^b(\vec{b} \cdot \hat{\Omega}, f) = \frac{-i}{3\sqrt{2}} \sin(f_n) e^{-i\frac{f_n}{3}(6+(\vec{a}-\vec{c}) \cdot \hat{\Omega})} \left[e^{-2if_n} \text{sinc}(f_n(1 + \vec{b} \cdot \hat{\Omega})) + \text{sinc}(f_n(1 - \vec{b} \cdot \hat{\Omega})) \right], \quad (15)$$

$$T_A^c(\vec{c} \cdot \hat{\Omega}, f) = \frac{-i}{3\sqrt{2}} \sin(f_n) e^{-i\frac{f_n}{3}(9+(\vec{b}-\vec{a}) \cdot \hat{\Omega})} \left[\text{sinc}(f_n(1 + \vec{c} \cdot \hat{\Omega})) + \text{sinc}(f_n(1 - \vec{c} \cdot \hat{\Omega})) \right], \quad (16)$$

nor does the variable E :

$$T_E^a(\vec{a} \cdot \hat{\Omega}, f) = \frac{1}{6\sqrt{6}} \left[\text{sinc}(f_n(1 + \vec{a} \cdot \hat{\Omega})) \left(e^{-i\frac{f_n}{3}(9+(\vec{c}-\vec{b}) \cdot \hat{\Omega})} + e^{-i\frac{f_n}{3}(3+(\vec{c}-\vec{b}) \cdot \hat{\Omega})} - 2e^{-i\frac{f_n}{3}(15+(\vec{c}-\vec{b}) \cdot \hat{\Omega})} \right) + \text{sinc}(f_n(1 - \vec{a} \cdot \hat{\Omega})) \left(2e^{-i\frac{f_n}{3}(3+(\vec{c}-\vec{b}) \cdot \hat{\Omega})} - e^{-i\frac{f_n}{3}(15+(\vec{c}-\vec{b}) \cdot \hat{\Omega})} - e^{-i\frac{f_n}{3}(9+(\vec{c}-\vec{b}) \cdot \hat{\Omega})} \right) \right], \quad (17)$$

$$T_E^b(\vec{b} \cdot \hat{\Omega}, f) = \frac{1}{6\sqrt{6}} \left[\text{sinc}(f_n(1 + \vec{b} \cdot \hat{\Omega})) \left(e^{-i\frac{f_n}{3}(15+(\vec{a}-\vec{c}) \cdot \hat{\Omega})} + e^{-i\frac{f_n}{3}(9+(\vec{a}-\vec{c}) \cdot \hat{\Omega})} - 2e^{-i\frac{f_n}{3}(3+(\vec{a}-\vec{c}) \cdot \hat{\Omega})} \right) + \text{sinc}(f_n(1 - \vec{b} \cdot \hat{\Omega})) \left(2e^{-i\frac{f_n}{3}(15+(\vec{a}-\vec{c}) \cdot \hat{\Omega})} - e^{-i\frac{f_n}{3}(9+(\vec{a}-\vec{c}) \cdot \hat{\Omega})} - e^{-i\frac{f_n}{3}(3+(\vec{a}-\vec{c}) \cdot \hat{\Omega})} \right) \right], \quad (18)$$

$$T_E^c(\vec{c} \cdot \hat{\Omega}, f) = \frac{1}{6\sqrt{6}} \left[\text{sinc}(f_n(1 + \vec{c} \cdot \hat{\Omega})) \left(e^{-i\frac{f_n}{3}(3+(\vec{b}-\vec{a}) \cdot \hat{\Omega})} + e^{-i\frac{f_n}{3}(15+(\vec{b}-\vec{a}) \cdot \hat{\Omega})} - 2e^{-i\frac{f_n}{3}(9+(\vec{b}-\vec{a}) \cdot \hat{\Omega})} \right) + \text{sinc}(f_n(1 - \vec{c} \cdot \hat{\Omega})) \left(2e^{-i\frac{f_n}{3}(9+(\vec{b}-\vec{a}) \cdot \hat{\Omega})} - e^{-i\frac{f_n}{3}(15+(\vec{b}-\vec{a}) \cdot \hat{\Omega})} - e^{-i\frac{f_n}{3}(3+(\vec{b}-\vec{a}) \cdot \hat{\Omega})} \right) \right]. \quad (19)$$

III. NOISE SPECTRAL DENSITY

Until now we have only considered the gravitational wave contribution, $\psi_{ij}(t)$, to the time-varying part of the phase $\phi_{ij}(t)$. Our next task is to account for the instrument noise contributions. There are three main noise sources: the laser phase noise $C(t)$, the position noise $n^p(t)$ and the acceleration noise $n^a(t)$.

The total phase variation is given by

$$\Phi_{ij}(t) = C_i(t - L_{ij}) - C_j(t) + \psi_{ij}(t) + n_{ij}^p(t) - \hat{x}_{ij} \cdot [\vec{n}_{ij}^a(t) - \vec{n}_{ji}^a(t - L_{ij})]. \quad (20)$$

The position noise $n_{ij}^p(t)$ includes shot noise and pointing jitter in the measurement of the signal sent by spacecraft i and measured by the photo-detector in spacecraft j . The acceleration noise $\vec{n}_{ij}^a(t)$ is from the gravitation reference system in spacecraft j along the axis that points toward spacecraft i . The phase noise associated with the laser on spacecraft i is denoted $C_i(t)$. It is easy to show that the phase noise cancels in a rigid, non-rotating Sagnac interferometer. More complicated second generation Sagnac variables can be constructed to account for the rotation and flexing of the array[12, 13]. For simplicity we work with the basic Sagnac variables as they give results that are almost identical to those found using the second generation variables.

We assume that all the interferometer arms are of approximately equal length ($L = 5 \times 10^7$ m), and that the noise spectral densities $S_n(f)$ are similar on each spacecraft. The noise transfer functions are then given by

$$S_n^T(f) = 2[1 + 2\cos(2f_n)]^2 [S_n^p(f) + 4\sin^2(f_n)S_n^a(f)], \quad (21)$$

where according to the fiducial BBO design

$$\begin{aligned} S_n^p(f) &= \frac{2.0 \times 10^{-34}}{(3L)^2} \text{ Hz}^{-1}, \\ S_n^a(f) &= \frac{9.0 \times 10^{-34}}{(2\pi f)^4 (3L)^2} \text{ Hz}^{-1}. \end{aligned} \quad (22)$$

This expression for the Symmeterized Sagnac noise transfer function was previously derived in Refs. [7, 11]. The noise transfer functions in the A and E channel share the same form, as first pointed out in Ref. [7]:

$$S_n^A(f) = S_n^E(f) = 8\sin^2(f_n) \left[(2 + \cos(2f_n)) S_n^s(f) + 2(3 + 2\cos(2f_n) + \cos(4f_n)) S_n^a(f) \right] \quad (23)$$

IV. CROSS-CORRELATION OF TWO DETECTORS

The CGB signal can be extracted from the instrument noise by cross-correlating the outputs of two independent interferometers. The pair of co-planar interferometers of the BBO do not share any common components, so the noise in each detector should be largely

uncorrelated. Possible correlated sources of noise include solar flares and fluctuations in the refractive index of the inter-planetary medium. Another potential source of correlated noise is the residual from subtracting foreground sources such as double neutron star binaries [2, 3]. Here we will assume that any correlated sources of noise are well below the level of the CGB.

We assume that the CGB is stationary, Gaussian, isotropic, and unpolarized. The background can be expanded in terms of plane waves:

$$h_{ij}(t, \vec{x}) = \sum_A \int_{-\infty}^{\infty} df \int d\hat{\Omega} \tilde{h}_A(f, \hat{\Omega}) e^{-2\pi i f(t - \hat{\Omega} \cdot \vec{x})} \epsilon_{ij}^A(\hat{\Omega}), \quad (24)$$

where $\epsilon^A(\hat{\Omega})$ are polarization tensors given in term of the basis tensors

$$\begin{aligned} \epsilon^+(\hat{\Omega}, \psi) &= \mathbf{e}^+(\hat{\Omega}) \cos 2\psi - \mathbf{e}^\times(\hat{\Omega}) \sin 2\psi, \\ \epsilon^\times(\hat{\Omega}, \psi) &= \mathbf{e}^+(\hat{\Omega}) \sin 2\psi + \mathbf{e}^\times(\hat{\Omega}) \cos 2\psi. \end{aligned} \quad (25)$$

The basis tensors can be expressed in term of an orthonormal set of unit vectors \hat{m} , \hat{n} and $\hat{\Omega}$ as

$$\begin{aligned} \mathbf{e}^+(\hat{\Omega}) &= \hat{m} \otimes \hat{m} - \hat{n} \otimes \hat{n}, \\ \mathbf{e}^\times(\hat{\Omega}) &= \hat{m} \otimes \hat{n} + \hat{n} \otimes \hat{m}. \end{aligned} \quad (26)$$

From the strain

$$S(\hat{\Omega}, f, t) = \mathbf{D}(\hat{\Omega}, f) : (h^+(f, t, \vec{x}_0) \epsilon^+(\hat{\Omega}, \psi) + h^\times(f, t, \vec{x}_0) \epsilon^\times(\hat{\Omega}, \psi)), \quad (27)$$

we find that after averaging over polarizations, the cross-correlated signal of two detectors in the presence of such a background is given by

$$\langle S_1(t) S_2(t) \rangle = \int_0^\infty df S_h(f) R_{12}(f), \quad (28)$$

where $S_h(f)$ is the total power spectral density due to both polarizations:

$$S_h(f) = S_h^+(f) + S_h^\times(f), \quad (29)$$

and

$$R_{12}(f) = \sum_A \int \frac{d\Omega}{8\pi} F_1^{A*}(\hat{\Omega}, f) F_2^A(\hat{\Omega}, f). \quad (30)$$

The transfer function R_{12} is a purely geometric factor that accounts for the overlap of the antenna patterns of the two detectors. The antenna pattern functions F are given by

$$F^A(\hat{\Omega}, f) = \mathbf{D}(\hat{\Omega}, f) : \mathbf{e}^A(\hat{\Omega}). \quad (31)$$

The optimal signal-to-noise ratio squared is given by [4, 5]

$$\text{SNR}_C^2 = 2T \int_0^\infty df S_h^2(f) \frac{|R_{12}(f)|^2}{S_{n_1}(f)S_{n_2}(f)}. \quad (32)$$

where S_{n_1} is the noise spectral density of interferometer 1, S_{n_2} is the noise spectral density of for interferometer 2 and S_h is the spectral density of the CGB. A signal to noise ratio of $\text{SNR} = 3.3$ indicates that the CGB has been detected at 95% confidence, with a 5% false alarm probability [5].

The power spectral density of the CGB is related to the energy density in gravitational waves per logarithmic frequency interval, $\Omega_{gw}(f)$ (in units of the critical denisty), by

$$S_h(f) = \frac{3H_0^2}{4\pi^2} \frac{\Omega_{gw}}{f^3}. \quad (33)$$

Standard inflationary models predict that $\Omega_{gw}(f)$ will be roughly scale invariant, with an amplitude $\Omega_{gw} \sim 10^{-15}$ in the $f = 1$ Hz region.

The contribution to the cross-correlated SNR per logarithmic frequency interval can be written as

$$\frac{d \text{SNR}_C^2}{d \ln f} = \frac{h_{\text{opt}}^4(f)}{h_{\text{eff}}^4(f)} \quad (34)$$

where $h_{\text{eff}}(f)$ is the effective sensitivity curve

$$\tilde{h}_{\text{eff}}(f) = \sqrt{\frac{S_n(f)}{|R_{12}(f)|}} \quad (35)$$

and $h_{\text{opt}}(f)$ is the optimally filtered CGB signal

$$h_{\text{opt}}(f) = (2Tf)^{1/4} \sqrt{S_h(f)}. \quad (36)$$

These definitions are equivalent to the usual definitions used to plot sensitivity curves and gravitational wave signals for coherent gravitational wave sources. The main difference is that the optimally filtered signal strength grows as $T^{1/2}$ with coherent matched filtering, while it only grows as $T^{1/4}$ for cross-correlated stochastic signals.

V. NUMERICAL ANALYSIS

The optimal SNR for the BBO comes from combining the full set of independent interferometry channels in each of the two co-located detectors that form the star constellation:

$$\text{SNR}_{\text{opt}}^2 = \sum_{\alpha=A_1, E_1, T_1} \sum_{\beta=A_2, E_2, T_2} \text{SNR}_{\alpha\beta}^2. \quad (37)$$

Our first task is to calculate the geometrical overlap of each pair of channels, $R_{\alpha\beta}(f)$. The all-sky integral in (30) was performed numerically using the *HEALPIX* package [15]. Plots of the overlap factors are shown in Figures 1-6 for the standard BBO configuration in which the two overlapping detectors form a symmetric six pointed star. The plots show the R 's scaled by overall factors such as $\sin^2(f_n)$, which they share in common with the corresponding noise transfer functions.

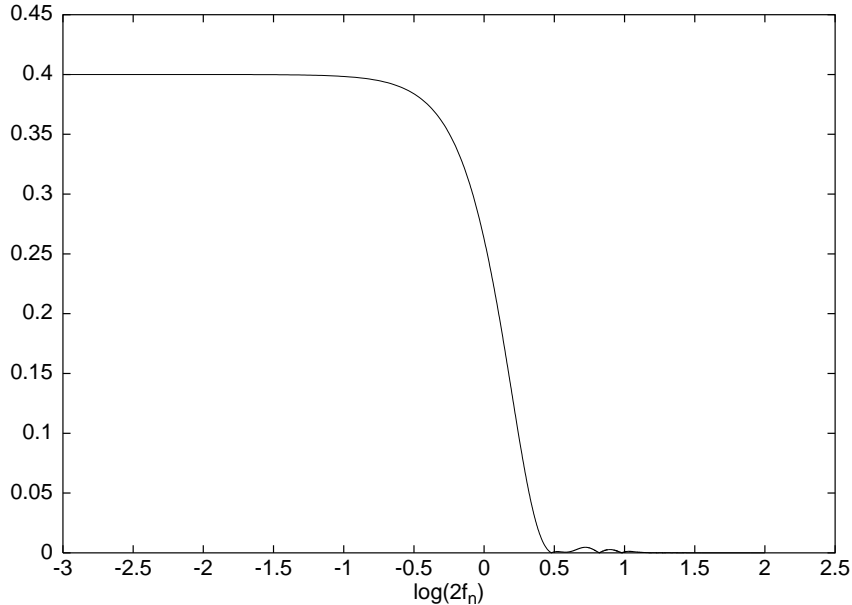


FIG. 1: $R_{12}(f_n)/\sin^2(f_n)$ for $A_1 \times A_2$

We expect R_{12} to vanish for the cross terms as the A , E and T channels are approximately signal orthogonal. In the low frequency limit the A and E can be shown [8] to be equivalent to Cutler's s_I and s_{II} [14] variables, which describe two Michelson detectors rotated by an angle $\pi/4$. Combining the geometrical factors R_{12} with the noise transfer functions leads to the effective sensitivity curves shown in Figures 7 and 8.

The combined effective sensitivity follows from the optimal signal to noise ratio (37). Figure 9 shows the combined sensitivity curve using all channel combinations plotted against the optimal CGB signal for a scale invariant spectrum with $\Omega_{gw} = 10^{-15}$.

An alternative way of conveying the information contained in Figure 9 is to plot $\text{SNR}(f) = (d\text{SNR}^2(f)/d\ln f)^{1/2}$: the contribution to the signal to noise ratio per logarithmic frequency interval. The optimal $\text{SNR}(f)$ for $\Omega_{gw} = 10^{-15}$ is shown in Figure 10.

The preceding graphs assumed that the two triangular interferometers formed a symmetrical six pointed star. However, one could consider alternative arrangements where the two

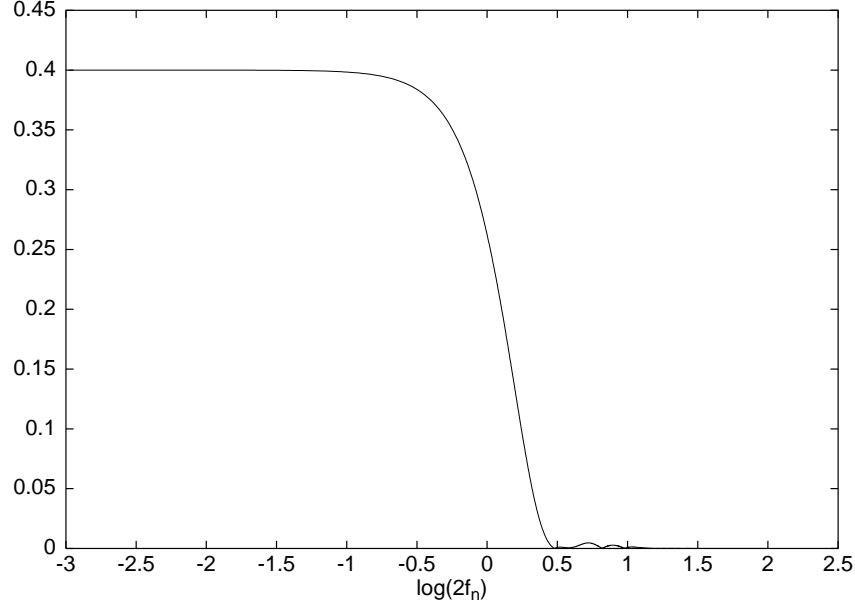


FIG. 2: $R_{12}(f_n)/\sin^2(f_n)$ for $E_1 \times E_2$

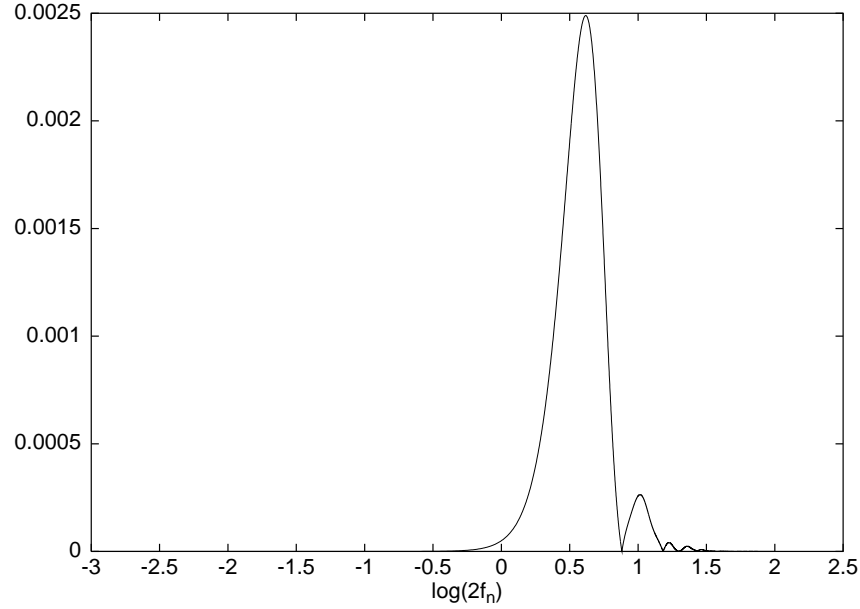


FIG. 3: $R_{12}(f_n)/(1 + 2\cos(2f_n))^2$ for $T_1 \times T_2$

detectors are rotated by an arbitrary angle λ with respect to one another. In our numbering convention for the vertices of each triangle the symmetric star corresponds to a rotation angle of $\lambda = \pi$. As we vary λ , the individual SNRs from $A_1 \times A_2$ and $E_1 \times E_2$ decrease, with minima at $\lambda = \pi/4$ and $\lambda = 3\pi/4$ as expected [11]. The SNR for $A_1 \times E_2$, on the other hand, increases, with maxima at $\lambda = \pi/4$ and $\lambda = 3\pi/4$. This behavior is illustrated in Figures 11 and 12. The net effect is that the optimal SNR is independent of the relative

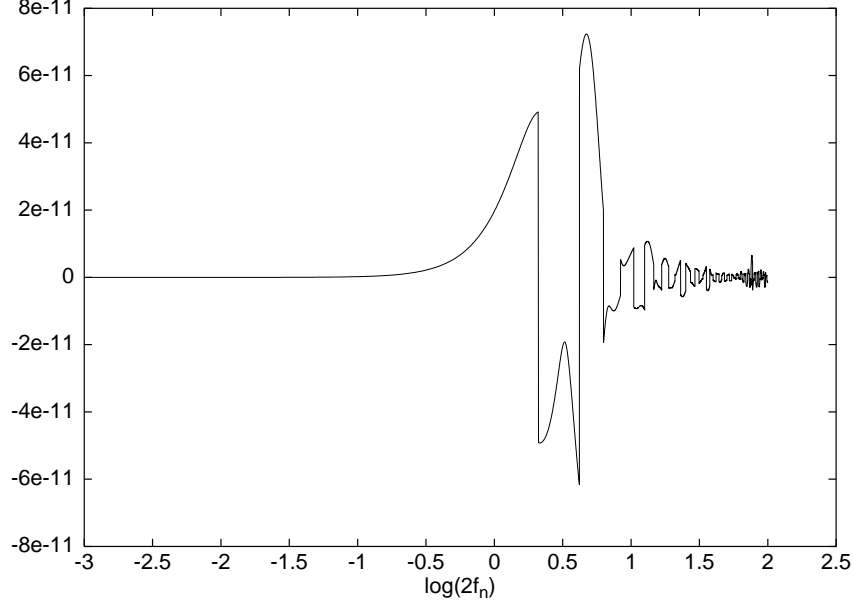


FIG. 4: $R_{12}(f_n)/((1 + 2 \cos(2f_n)) \sin(f_n))$ for $A_1 \times T_2$ or $T_1 \times A_2$

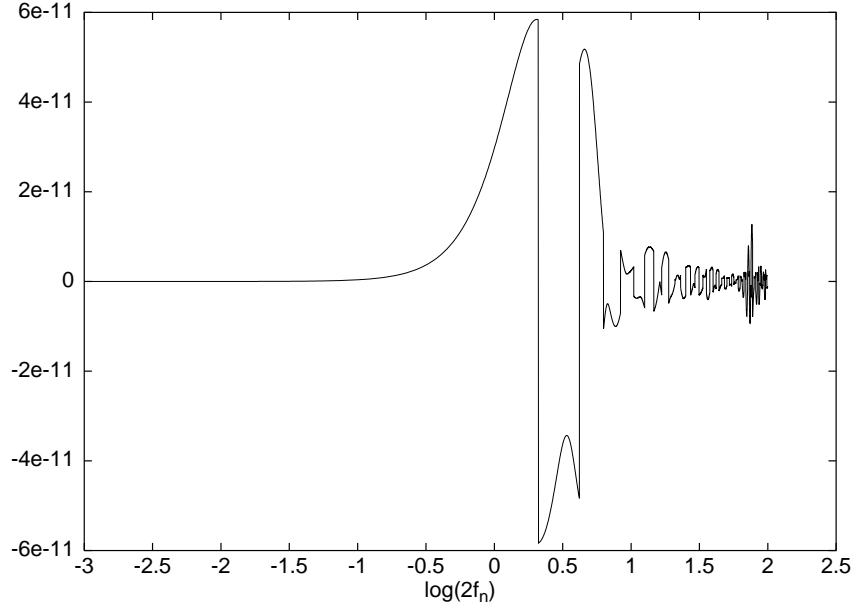


FIG. 5: $R_{12}(f_n)/((1 + 2 \cos(2f_n)) \sin(f_n))$ for $E_1 \times T_2$ or $T_1 \times E_2$.

orientation λ .

We find that the optimal SNR for scale invariant CGB that can be achieved by the fiducial BBO design is equal to

$$\text{SNR}_{\text{opt}} = 155 \sqrt{\frac{T}{5 \text{ yr}}} \frac{\Omega_{gw}}{10^{-15}} \left(\frac{H_0}{70 \text{ km s}^{-1} \text{ Mpc}^{-1}} \right)^2, \quad (38)$$

which is well above the 3.3 threshold mentioned in the introduction. Conversely, the

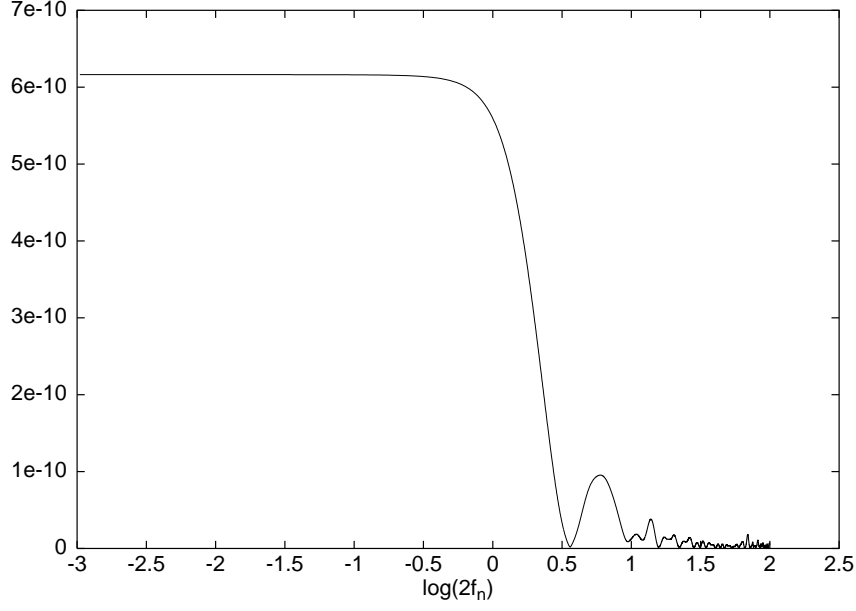


FIG. 6: $R_{12}(f_n)/\sin^2(f_n)$ for $A_1 \times E_2$ or $E_1 \times A_2$.

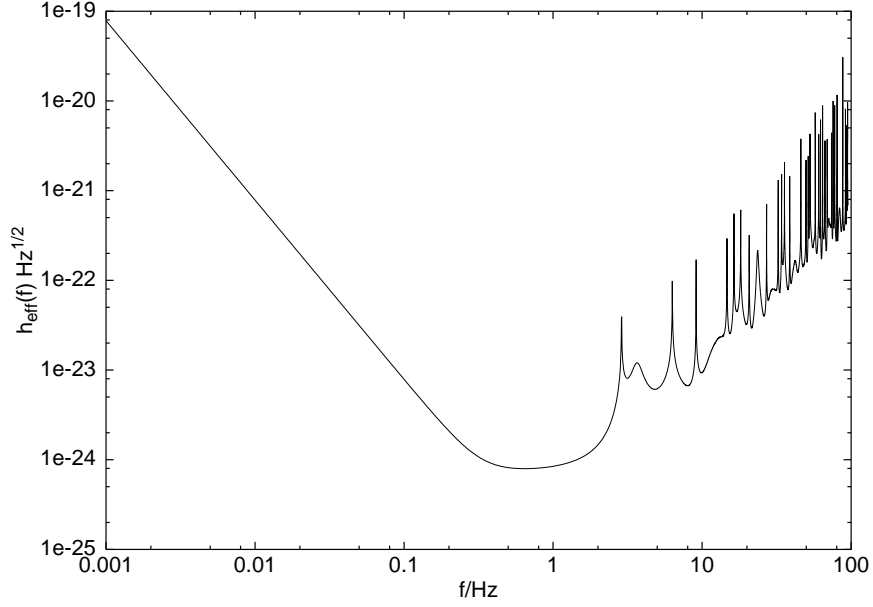


FIG. 7: Effective sensitivity for $A_1 \times A_2$ ($E_1 \times E_2$)

minimum Ω_{gw} for which we could detect the CGB with the 95% confidence is equal to $2.2 \times 10^{-17} (5\text{yr}/T)^{1/2} (70\text{ km s}^{-1} \text{ Mpc}^{-1}/H_0)^2$. Our findings agree with the recent independent calculation by Seto [16].

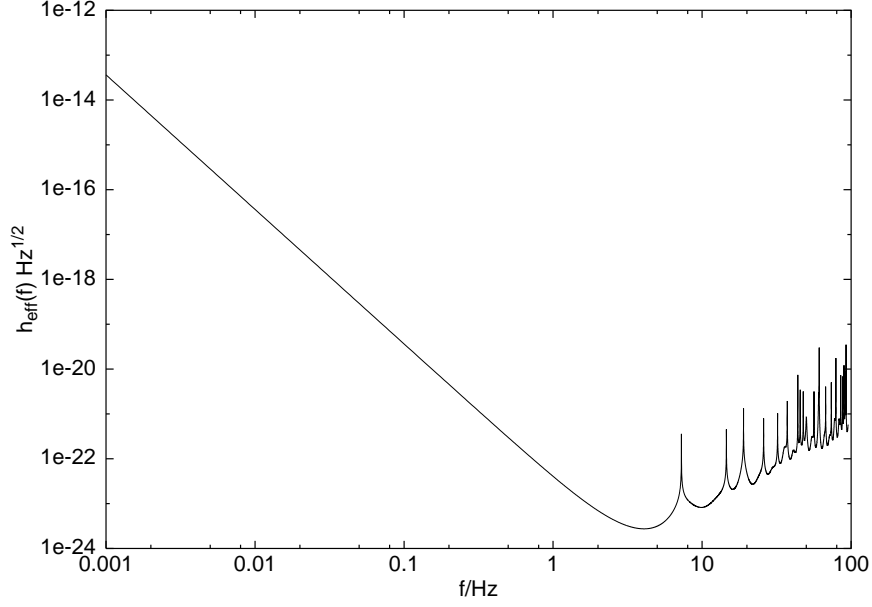


FIG. 8: Effective sensitivity for $T_1 \times T_2$

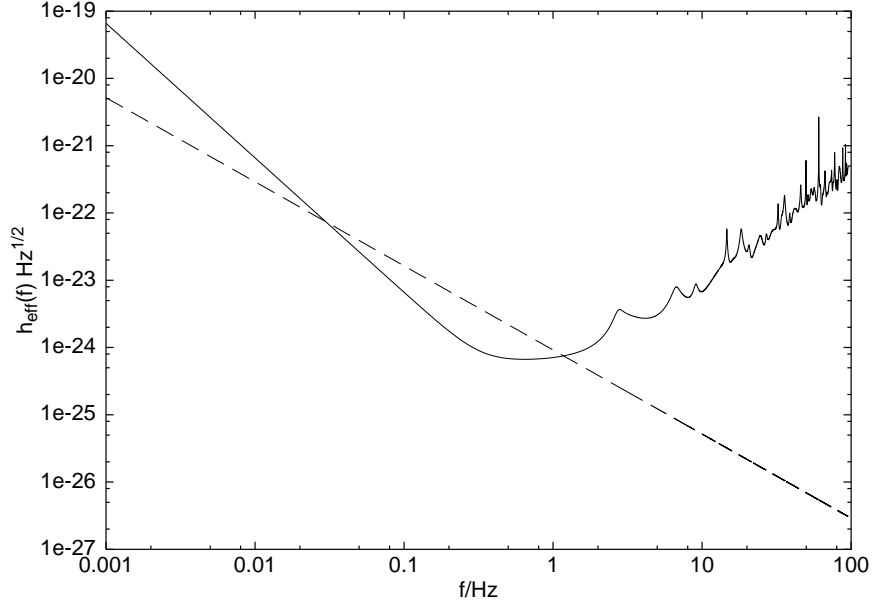


FIG. 9: The combined sensitivity curve (solid line) plotted against the optimal CGB signal (dashed line) for an observation time of $T = 1\text{yr}$.

VI. CONCLUSION

We have determined that the fiducial BBO design would be able to detect a scale invariant CGB with an energy density as low as $\Omega_{gw} = 2.2 \times 10^{-17} (5\text{yr}/T)^{1/2} (70 \text{ km s}^{-1} \text{ Mpc}^{-1}/H_0)^2$. We found that the optimal sensitivity is independent of the relative orientation of the co-

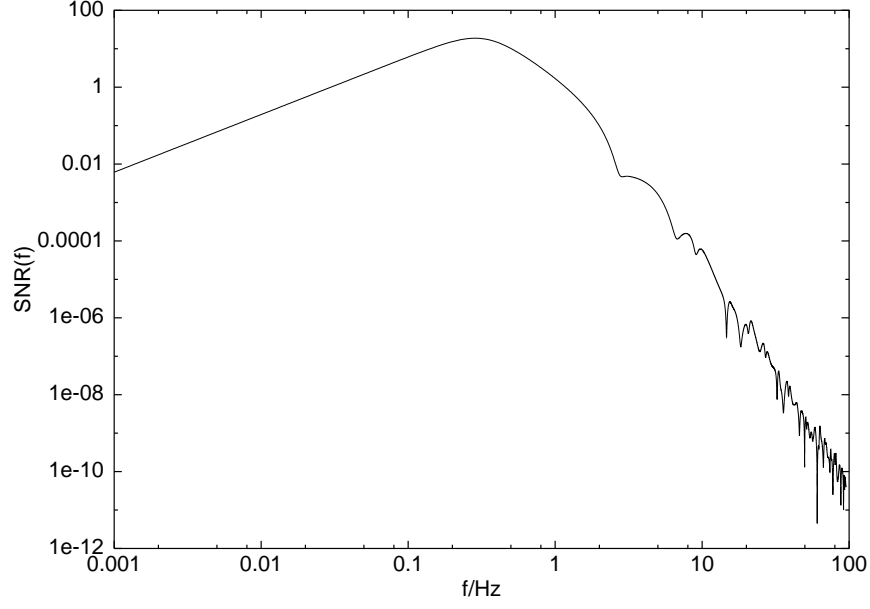


FIG. 10: Optimal $\text{SNR}(f)$

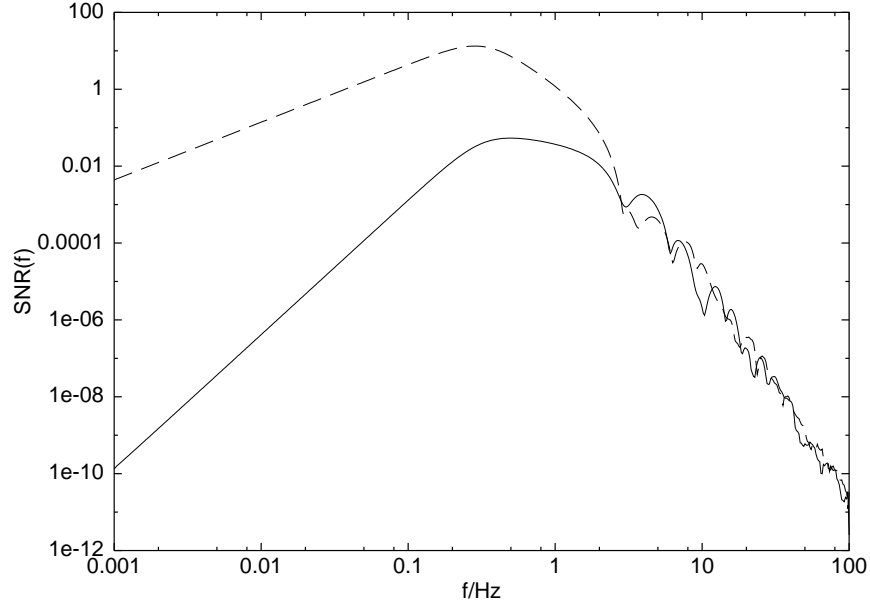


FIG. 11: $\text{SNR}_{A_1 A_2}(f)$ for an angle of $\lambda = \pi$ (dashed line) and $\lambda = \pi/4$ (solid line).

planar detectors used to perform the cross correlation.

-
- [1] T. L. Smith, M. Kamionkowski & A. Cooray, astro-ph/0506422 (2005).
 - [2] C. Cutler & J. Harms, gr-qc/0511092 (2005).
 - [3] N. Seto, N. J. Cornish & E. S. Phinney, gr-qc/xxx (2005).

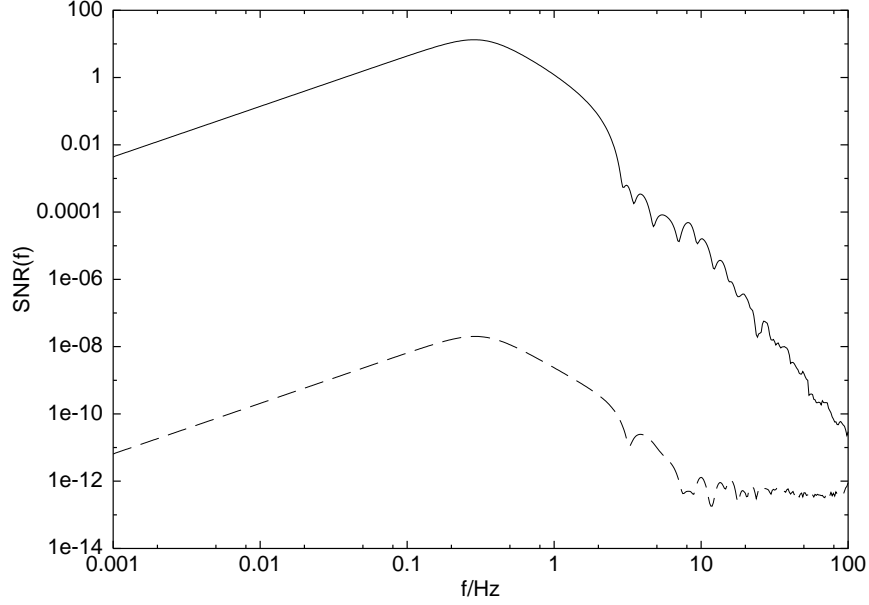


FIG. 12: $\text{SNR}_{A_1 E_2}(f)$ for an angle of $\lambda = \pi$ (dashed line) and $\lambda = \pi/4$ (solid line).

- [4] E. E. Flanagan, Phys. Rev. D**48**, 2389 (1993).
- [5] B. Allen & J.D. Romano, Phys. Rev. D**59**, 102001 (1999).
- [6] S. Phinney *et al.*, *The Big Bang Observer: Direct detection of gravitational waves from the birth of the Universe to the Present*, NASA Mission Concept Study (2004).
- [7] T. A. Prince, M. Tinto, S. L. Larson & J. W. Armstrong, Phys. Rev. D **66**, 122002 (2002).
- [8] J. Crowder & N. J. Cornish Phys. Rev. D, (2005).
- [9] N. J. Cornish & S. L. Larson Class. Quantum Grav.**18**, 3473 (2001).
- [10] C. Ungarelli & A. Vecchio, Rev. D**64**, 121501 (2001).
- [11] N.J. Cornish, Phys. Rev. D**65**, 022004 (2001).
- [12] N. J. Cornish & R. W. Hellings Class. Quantum Grav.**20**, 4851 (2003).
- [13] D. A. Shaddock, M. Tinto, F. B. Estabrook & J. W. Armstrong, Phys. Rev. D**68**, 061303 (2003).
- [14] C. Cutler, Phys. Rev. D**57**, 7089 (1998).
- [15] K. M. Gorski, B. D. Wandelt, E. Hivon, F. K. Hansen & A. J. Banday,
<http://healpix.jpl.nasa.gov/>.
- [16] N. Seto gr-qc/0510067 (2005).